Feasibility study on a robot-assisted procedure for tumor localization using needle-rotation force signals

Xiaoyu Liu[1], Hongqiang Huo[1], Lizhen Wang[1], Yuanjie Zhu[1], Aoran Sun[4], Wei Yao*[3], and YuboFan*[1,2]

[1] Key Laboratory for Biomechanics and Mechanobiology of Ministry of Education, School of Biological Science and Medical Engineering, Beihang University, Beijing, 100191, PR China

[2] National Research Center for Rehabilitation Technical Aids, Beijing 100176, PR China

[3] Department of Biomedical Engineering, University of Strathclyde, Glasgow G40NW, United kingdom

*Corresponding authors:

Dr. Wei Yao, , E-mail: w.yao@strath.ac.uk

Address: Wolfson Center, University of Strathclyde, 106 Rottenrow, Glasgow G40NW, UK

Prof. Yubo Fan, Tel: 0086-10-8233-9428, E-mail: yubofan@buaa.edu.cn

Address 1: Yifu Building, Beihang University, 37#Xueyuan Road, Haidian District, Beijing, 100191, China

Address 2: 1#Ronghuazhong Road, Daxing District, Beijing, 100176, China

Abstract: Accurate tumor localization is critical to early-stage cancer diagnosis and therapy. The recent force-guided technique allows to determine the depth of a suspicious tumor on the insertion path, while the spatial localization is still a great challenge. In this paper, a novel robot-assisted procedure was proposed to identify special tumor location using force signals during needle rotation. When there is a harder tumorous tissue around the needle rotation, an abnormal force signal will point to the location of the suspicious tissue. Finite element simulation and phantom experiment were conducted to test the feasibility of the procedure for the tumor localization. The simulation results showed that the harder tumorous tissue made a significant difference on the stress and deformation distributions for the surroundings, changing the needle-rotation force signal when the needle rotated towards the harder tissue. The experimental results indicate that the direction of the tumor location can be identified by rotation-needle force signals. The intersection point of the two identified directions, derived from force signals of twice needle rotation, determined the tumor location ultimately. Also, parametric sensitivity tests were performed to examine the effective distance of the tumor location centre and the needle insertion point for the tumor localization. This procedure is expected to be used in robot-assisted system for cancer biopsy and brachytherapy.

Key words: Tumor localization; Robot-assisted procedure; Needle force; Finite element simulation; Phantom experiment.

1. Introduction

Effective early-stage diagnosis and therapy of cancer is critical to prevent disease development. Although digital rectal examination (DRE) has been commonly used to detect suspicious tumor tissue, a patient can be diagnosed with cancer only by needle biopsy, in which the suspicious tissue is removed by needle for further examination [1]. For the cancer therapy, brachytherapy is commonly used to treat early-stage cancer, in which radioactive sources are placed close to the tumor for radiotherapy [2]. Thus, accurate localization of the tumor is important to cancer diagnosis and therapy.

Recent advances in robot-assisted minimally invasive surgery (MIS) provided intelligent technology for tumor localization. Guided by Transrectal ultrasound (TRUS) or magnetic resonance imaging (MRI), a needles can be driven by a robotic manipulator to reach the target location [3-8]. Although image-guided technology have many appealing merits, there are still challenges for accurate localization. For example, TRUS is limited by its poor imaging quality, which reduces the detection rate significantly [9, 10]. MRI can provide higher spatial solution, but a metal needle inevitably generates a susceptibility artifact that would misguide the needle insertion and probably damage the normal tissue [11, 12].

To allow more accurate localization, force-guided technique has been proposed to assist TRUS and MRI navigation in robotic MIS [13-16]. This technique is based on the biomechanical theory that tumor tissue increases its induration and becomes harder than the normal tissue [17-20]. The harder tumor tissue would make a difference on the needle force signal, which can be used to identify the tumor location. The needle-tissue

force interaction has been investigated in the previous studies. Brett et al [21, 22] performed pioneering work on characterization of needle force to identify the type of tissue that on the needle insertion path. Kataoka et al [23] measured tip and friction needle forces when a needle is penetrating into a prostate. Okamura et al [24, 25] developed a mathematical model to simulate needle insertion mechanics, in which tissue stiffness, needle friction and puncture were computed. The model has also been used in surgical simulation and robot-assisted surgery. Majewicz et al [26] evaluated needle insertion forces using various needle types in ex vivo and in vivo experiments. Yan et al [27, 28], for the first time, proposed a force-guided technique for tumor detection using insertion forces in the prostate brachytherapy. By patients' experiments, they validated the effectiveness of the force-guided technique for prostate cancer detection.

However, the force-guided this technique only provides the depth of the suspicious tumor which is just on the path of insertion, spatial localization of a tumor uisng needle force is a significant challenge. In this paper, we proposed a novel robot-assisted procedure for tumor localization using needle-rotation forces signals. This procedure can predict the planar location of a suspicious tumor, which was validated using finite element simulation and phantom experiments. Also, we evaluated the effective range of needle-rotation localization in parametric tests. The proposed procedure is expected to use in robot-assisted guidance system for tumor localization.

2. Materials and methods

2.1Procedure description

The procedure of the force-guided tumor localization refers to 3 needle motions: vertical insertion, planar deviation and 360-degree rotation. The needle forces in three directions (F_x, F_y and F_z) are recorded during the needle motion. The tumor's location can be determined according to the force signals. The setup of the tumor localization procedure is illustrated in Fig. 1.
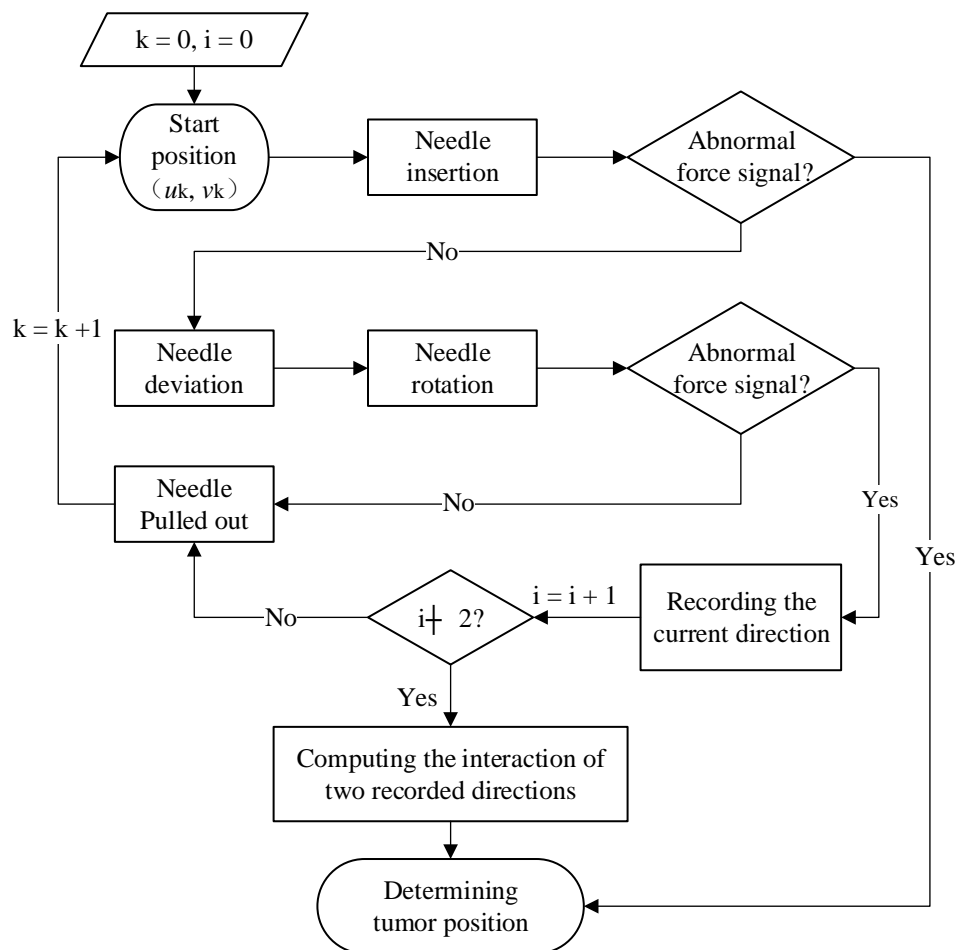

Fig. 1. The setup of robot-assisted tumor localization procedure using needle force signals

The main steps in the tumor localization procedure is elaborated as follows.

Step 1: A needle is driven to insert a suspicious tissue vertically (Fig. 2a). When abnormal signals is found in insertion force (F_z), it is considered that the tumor is located on the path of needle insertion. The method for analyzing and determining the depth of the tumor can be found in the literature by Yan *et al* [28].

Step 2: If there is no indication of abnormal signal during the insertion (Fig. 2b), the needle is then driven to perform a deviation in *x-y* plane (Fig. 2c), followed by a 360-degree rotation around the insertion axis (Fig. 2d). Normally, the rotation force ($F_r = \sqrt{F_x + F_y}$) as the needle motion exhibits smoothness. If there is a harder tumor around the needle, an abnormal force signal could be found when the needle rotates close to the tumor's location (Fig. 2e). The direction of the tumor's location relative to the insertion position can be identified according to the orientation of the abnormal signal (Fig. 2e).

Step 3: The needle is pulled out and driven to insert the suspicious tissue at a different position (2nd insertion position), repeating Step 1. If there is no harder tumor on the path of needle insertion, the needle is then driven to perform a deviation and a 360-degree rotation, repeating *Step 2*. The direction of the tumor's location relative to the 2nd insertion position can be identified in the second needle rotation (Fig. 2f). The location of the tumor is finally determined, which is the intersection of the two direction lines.
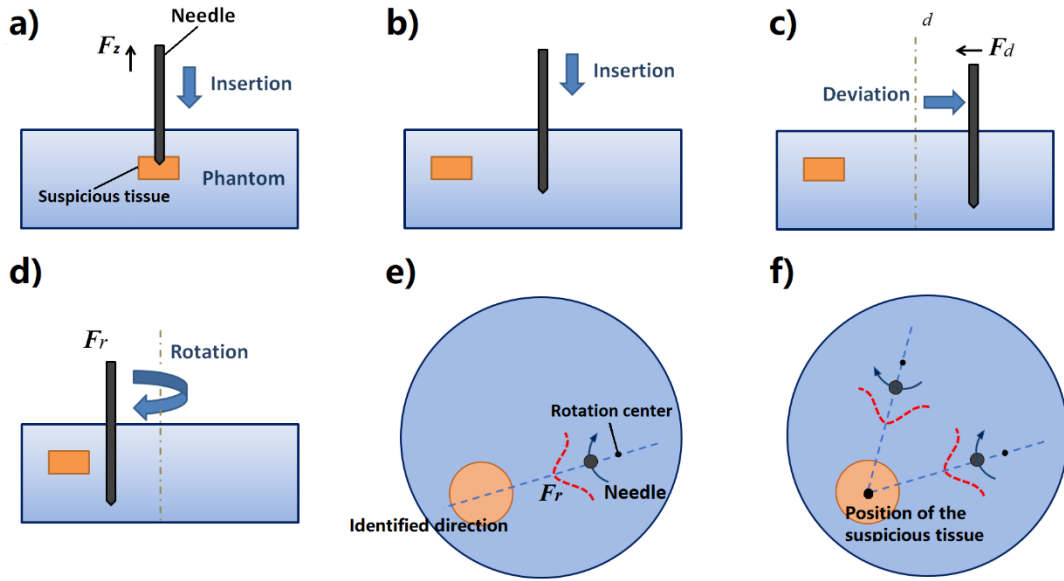
Fig. 2 Main steps in the robot-assisted procedure of tumor localization using needle force signals.

2.2 Evaluation by Finite element simulation

Finite element (FE) simulation was conducted to evaluate the feasibility of the rotation force-guided procedure for tumor localization. The simulation was performed with a 2D model in ANSYS 14.0 (ANSYS Inc., Canonsburg, PA) The 2D model includes a normal soft tissue ($D = 30$ mm), a tumor tissue ($D = 5$ mm) and a needle ($D = 1$ mm), shown in Fig. 2. The distance between the tumor center and the needle is 6 mm. Quadrangular elements were used for meshing the 2D model, since tetrahedron elements tend to exhibit mesh locking for large deformation. The contact relationship between the soft tissue and the needle was defined to be 'frictionless'. The normal tissue and tumor tissue were grouped into a 'multibody part' to permit their node-sharing. The movement of the normal tissue boundary is limited. In the simulation, the needle perform a planar deviation, followed by a 360-degree rotation, shown in Fig. 3.
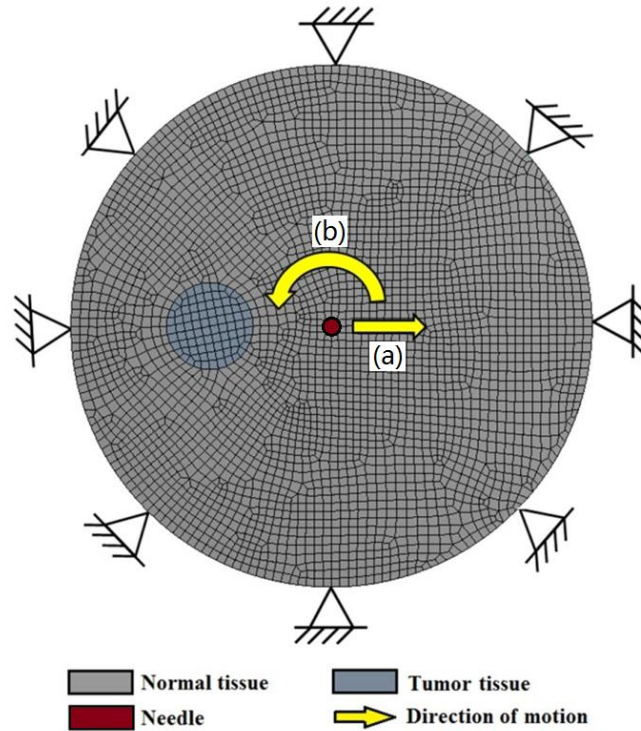
Fig. 3. A planar FE model representing a slice of a human prostate, a tumor and a needle. The yellow arrows represent the motions of the needle: (a) deviation and (b) 360-degree rotation.

The tissues in this model were treated as linear elastic materials, in which the elastic modulus of the tumor was set to 75 kPa that is five times of the normal tissue (15 kPa). The needle was modeled as a rigid body, since its deformation was insignificant. The parameters of the model are listed in Table 1.

Table 1 Geometries and material properties in the FE simulation

	D (mm)	NN	NE	E (kPa)	μ
Soft tissue	30	3152	3037	15	0.49
Tumor	5	109	92	75	0.49
Needle	1	9	4	—	—

Where: D, Diameter; NN, Number of nodes; NE, Number of elements; E, Elastic modulus; μ, Poinson's ratio.

2.3 Validation by phantom experimental test

An experimental test was conducted to further validate the proposed procedure for tumor localization. Considering simple and controllable environments provided by phantom experiment (e.g. mechanical properties and boundary conditions) [25], phantom rather than biological tissue was used in the current experiment. A silicone phantom with an embedded rubber button was made for the samples. The silicon with elastic modulus of ~15 kPa was used to simulate a normal tissue. The rubber with a elastic modulus of ~75 kPa was used to simulate a hard humor. Such material properties were considered because it has been reported that the elastic modulus of the tumor tissue is three to seven times than that of the normal tissue [17-20]. A commercial 7-DOF robotic manipulator (Cyton Gamma 1500, Robai Corporation, MA) was used to drive a needle to perform insertion, deviation and rotation. A 6-axis force/torque sensor (Nano17, ATI Industrial Automation, US), mounted between the end of the manipulator and the needle, was used to measure the interactive forces. The setup of the phantom experiment is shown in Fig. 4.

The experimental procedure is described as follow. First, the needle was driven to insert into the phantom sample vertically at a velocity of 1 mm/s. The distance between the insertion axis and the center of the "rubber tumor" is about 5 mm. And the needle was driven to perform a 2.5-mm deviation toward any direction at a velocity of 1mm/s. Then, the needle was driven to perform a 360-degree rotation around the insertion axis at a velocity of 1mm/s. After finishing the first rotation, the needle was pulled out the and performed the second rotation at a different insertion position. The data of needle force

vs. degree during the two needle rotations were recorded in real time.
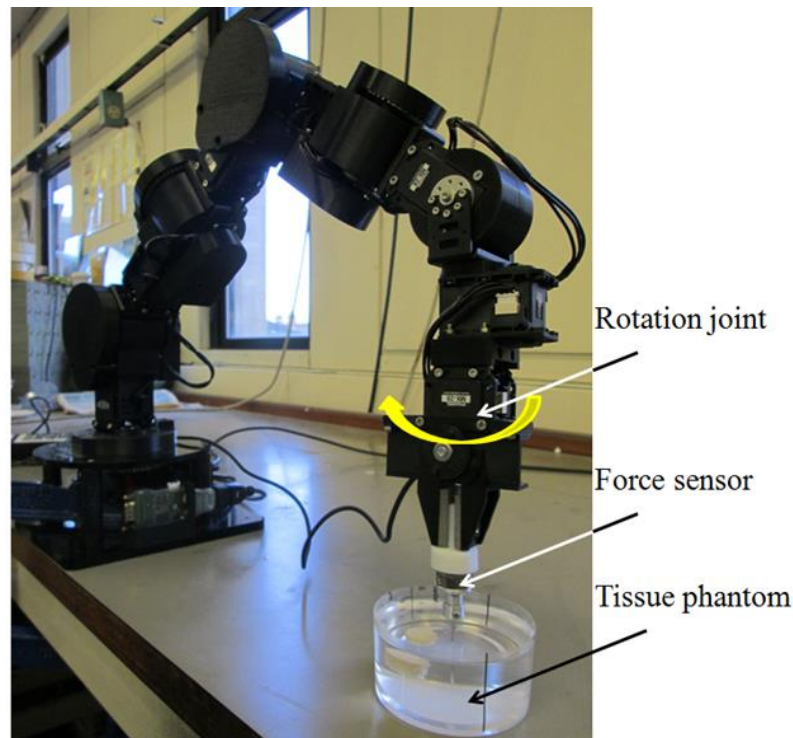
Fig. 4. The setup of the phantom experiment: A 7-DOF robotic manipulator was used to drive a needle to interact with the phantom tissues; A 6-axis force/torque sensor was used to measure real-time needle forces.

2.4 Parametric sensitivity test for the experiment

A parametric sensitivity test was conducted to evaluate the effectiveness of the localization procedure to the distance between the tumor centre and the needle insertion position (TC-IP). In this parametric test, five different distances were considered, which are 4, 6, 8, 10, and 12 mm. For each TC-IP distance, ten tests were performed to evaluate the effective range of tumor localization by this force-guided robotic procedure. The ratio of the maximum value to the average value of the needle force in a 360-degree rotation was used to indicate the sensitivity of the tumor localization.

3. Results

3.1 Evaluation by finite element simulation

The deformations and stress distributions of the tissue during needle rotation are shown in Fig. 5. The two figures indicate that the harder tumor made significant differences in the deformations and stress distributions, especially when the needle approached toward the tumor tissue.
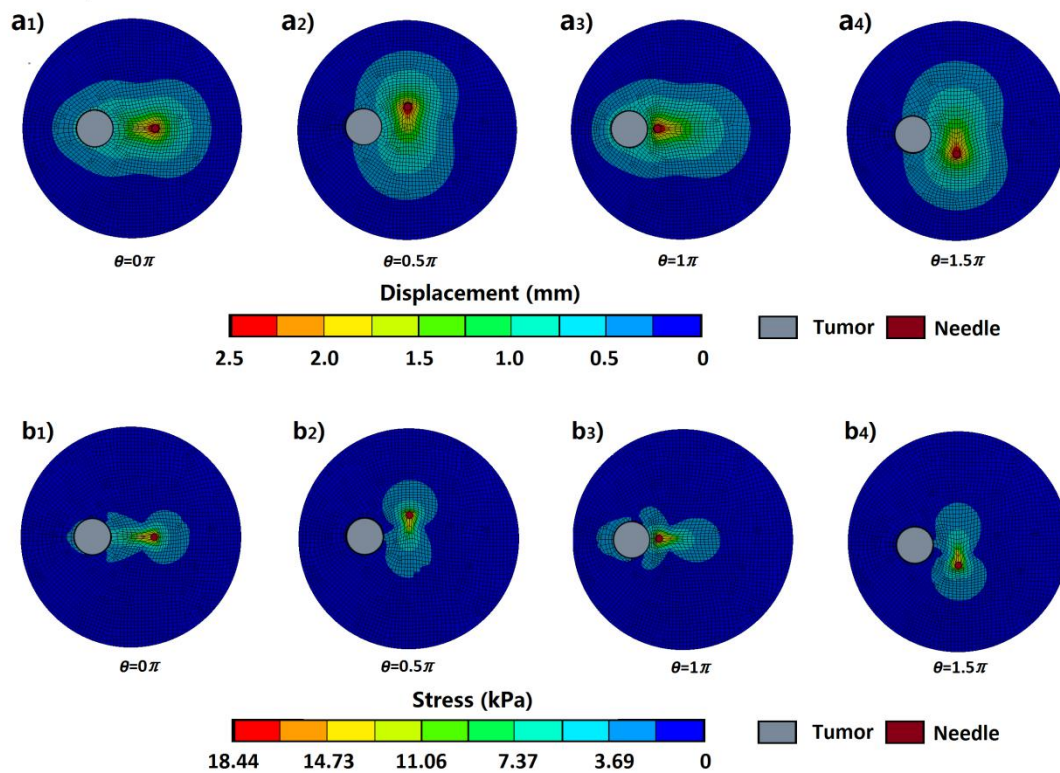

Fig. 5 Simulation of the deformation (Subfigure a1~a4) and equivalent stress (Subfigure b1~b4) distributions in the tissue when the needle is rotating (θ). The maximal deformation is 2.5 mm and the maximal equivalent stress is 18.436 kPa.

The resultant force (F_x, F_y and F_r) on the needle varying with the rotation degree (from 0 to 360 degrees) is illustrated in Fig. 6. The rotation force ($F_r = \sqrt{F_x + F_y}$) reached the maximum value (5.49 N) when the needle just moved toward the position of the tumor. Also, a greater force (5.23 N) appeared again when the needle moved opposite the

position of the tumor. It indicates that the direction of the tumor position can be identified by the characterization of the needle force curve during needle rotation.
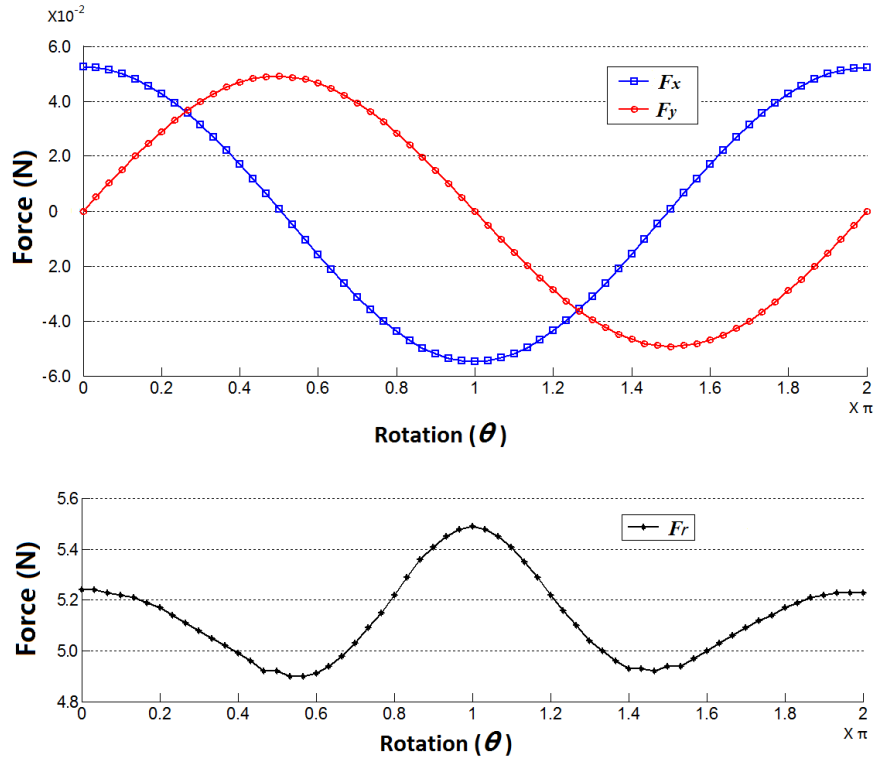
Fig. 6 The needle forces (F_x, F_y and F_r) varying with rotation degree. ($F_r = \sqrt{F_x + F_y}$)

3.2 Validation by phantom experiment

The accurate location of a tumor can be determined by performing two needle rotation procedures. Fig. 7 shows the curves of needle force vs. rotation degree in the two rotations. The degree for the maximum needle force in the first rotation is $\theta_1 = 1.31\ \pi$ (Fig. 7a), which points to the direction of the tumor location relative to the first insertion position. The degree for the maximum needle force in the second rotation is $\theta_2 = 0.70\ \pi$ (Fig. 7b), which points to the direction of the tumor location relative to the second insertion position.
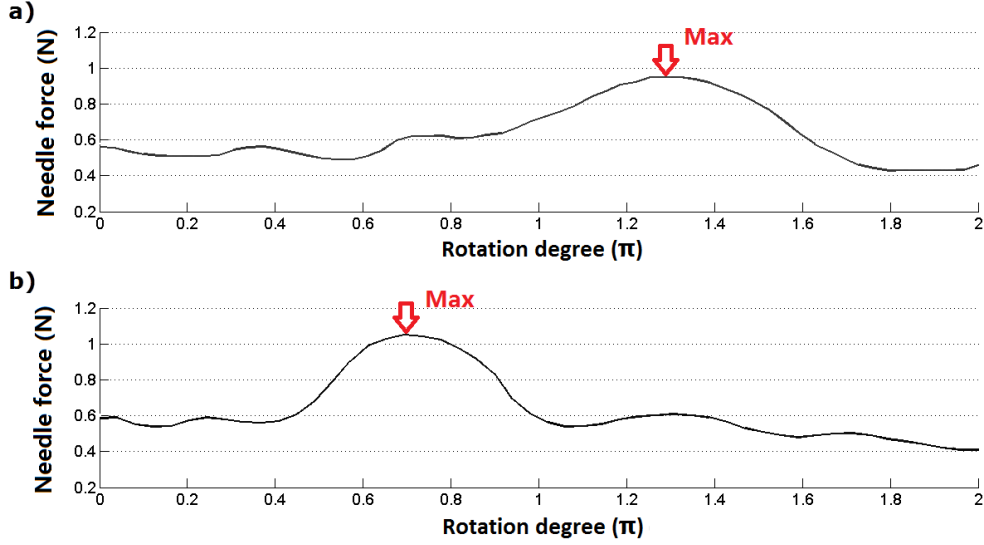
Fig. 7. The curves of needle force vs. rotation degree in a) the first insertion point and b) the second insertion point. (The force signals have been filtered.)

In order to illustrate the determination of the tumor location, the curve of the needle force vs. rotation degree was mapped as a contour plot, in which the color indicates the force value. The contour plots of the needle force for two rotations are shown in Fig. 8. It should be noted that the force value in the contour plot was moralized, in which all the force data was divided by the maximal value. The tumor location can be determined as the intersection of the two identified direction lines (P_0), which is the solution of the following equations:
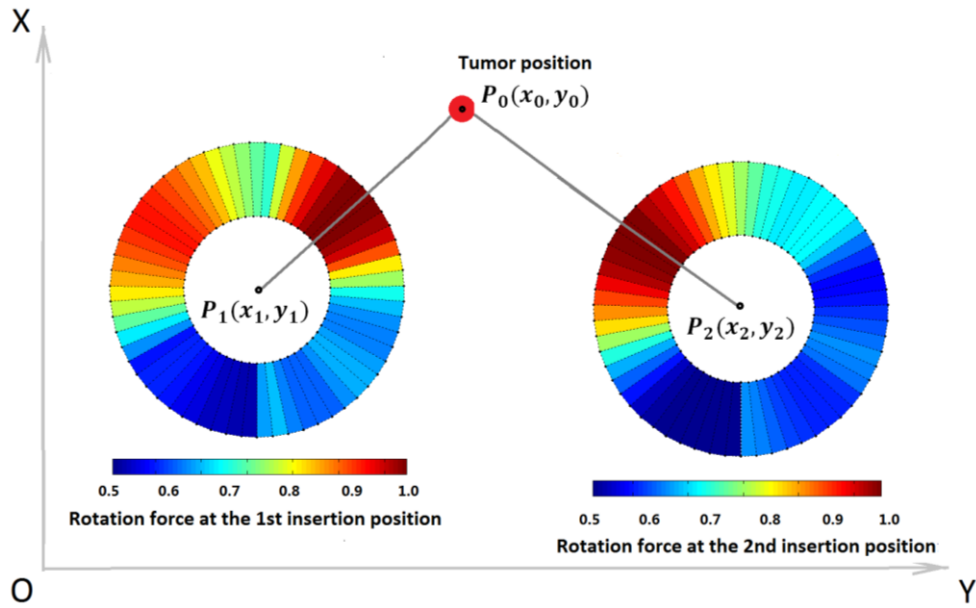
$$\begin{cases} x \cdot \tan\theta_1 + (y_1 - x_1) = y \\ x \cdot \tan\theta_2 + (y_2 - x_2) = y \end{cases}$$

where, $P_1(x_1, y_1)$ is the first insertion position; $P_2(x_2, y_2)$ is the second insertion position.

The $P_0(x_0, y_0)$ can be determined as:

$$x_0 = \frac{(y_2 - x_2) - (y_1 - x_1)}{\tan\theta_1 - \tan\theta_2},$$

$$y_0 = \frac{(y_2 - x_2) \cdot \tan\theta_1 - (y_1 - x_1) \cdot \tan\theta_2}{\tan\theta_1 - \tan\theta_2}$$

Fig. 8. The mapping of tumor localization using rotation forces by two needle rotation procedures. The Tumor position is determined to be the intersection of the two direction lines.

3.3 Parametric sensitivity test for the experiment

Five different distances (4, 6, 8, 10, and 12 mm) between the tumor centre and the insertion point (TC-IP) were considered in the sensitivity tests. For each TC-IP distance, 10 sensitivity tests were performed, in which the relation between the max/average ratio and the localization rate was evaluated (Fig. 9). The results indicate that the effective range of tumor localization by needle rotation force is within 8 mm TC-IP distance.
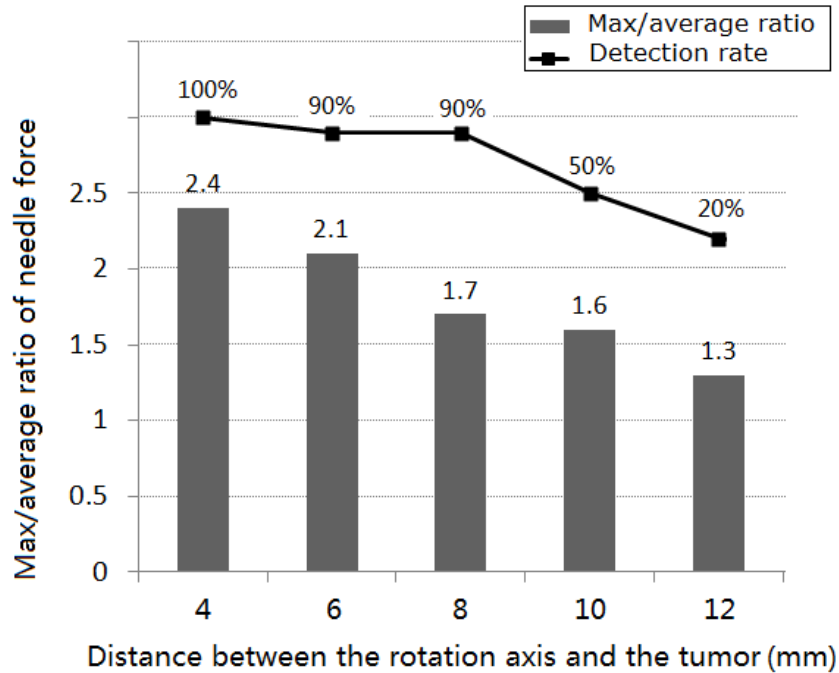
Fig. 9. The max/average ratio and success rate for the different distances between the rotation axis and the tumor.

4. Discussion

As an effective aided navigation approach, force-guided technique has been used in robot-assisted MIS [13-16]. This technique is based on the biomechanics that tumor tissue increases the induration and becomes harder than the normal tissue. Previous studies have indicated that tumor tissue has a more crowded structure and glandular pattern than the normal tissue, which increases its density and stiffness [17-20]. Changes in the composition and micro structure of the living tissue produce a significant difference in its mechanical properties. Moreover, with the tumor's growth, the surroundings produce more collagen to repair the damages caused by the invasion of tumorous cells. It is similar to the stromal reaction in the process of wound repair, leading to excessive collagen deposition and stiffening the surrounding tissue. The

stiffened tissue shows a significant difference in mechanical properties, allowing for tumor localization using force-guided robotic technology. In this paper, we propose a novel robot-assisted procedure for tumor localization according to needle-rotation force signals, which was validated by finite element simulation and phantom experiments.

Actually, the force-guided procedure for tumor localization is an invasive procedure, which would cause damage for the normal tissue. For the needle rotation in living tissue, increasing the rotation range (diameter) would definitely improve the accuracy of the localization rate, but it would also increase the incidence of tissue damage. Our preliminary experiment on living tissues has indicated that a 5-mm-diameter needle rotation doesn't damage the normal tissue. Since a larger range of rotation would damage the surrounding tissue, the needle rotation in a diameter of 5 mm is recommended for the range of the localization procedure.

Due to complicated situations in living tissue, it is a great challenge for the experimentally validated force-guided technology used into clinical surgery. Patient-specific factors such as age, anatomy, clinical stage and medical history would make significant differences in the mechanical properties of tumorous and normal tissues in the prostate. The proposed force-guided technology is based on the relative difference of needle forces applied by the harder tumor and the normal tissue. Therefore, patient-specific factors have little effect on the tumor identification for the current procedure. Still, much work will be needed on *ex vivo and in vivo* animal and human experiments in future studies. In our study, a 7-DOF robotic manipulator was used to perform needle motion including vertical insertion, deviation and 360-degree rotation. This commercial

robotic manipulator was designed to imitate a human arm. Although the robotic manipulator is able to complete the required needle motions, the 7-DOF joints are redundant for the current procedure. In future research, we would attempt to design a special and simplified robot to perform the tumor localization procedure more effectively.

In conclusion, we have proposed a novel robot-assisted procedure of needle rotation aiming to achieve tumor localization in the prostate. We used finite element simulation and phantom experiments to validate the proposed procedure. The simulation results showed that the harder timorous tissue affected the stress distribution in the surrounding tissue during needle rotation. The phantom experiment indicated that the tumor's location can be predicted by means of two needle rotations in different points. These results are promising for further research be means of *ex vivo and in vivo* animal and human experiments using the proposed procedure. The current procedure is expected to be used in robot-assisted systems for prostate biopsy and brachytherapy.

Conflict of interest statement

None.

References

[1] J. C. Presti, Prostate cancer: assessment of risk using digital rectal examination, tumor grade, prostate-specific antigen, and systematic biopsy, J. Radiol. Clin of North Amer. 38(January (1)) (2000) 49-58.

[2] S. E. Langley, R. Laing, Prostate brachytherapy has come of age: A review of the technique and results, J. BJU Int. 89(February (3)) (2002)241-249.

[3] A. Krieger, R. Susil, C. Menard, J. Coleman, G. Fichtinger, E. Atalar, and L. Whitcomb, Design of a novel MRI compatible manipulator for image guided prostate interventions, IEEE Trans. Biomed. Eng. 52 (February (2)) (2005) 306-313.

[4] G. Fichtinger, E. C. Burdette, A. Tanacs, A. Patriciu, D. Mazilu, L.L. Whitcomb, and D. Stoianovici, Robotically assisted prostate brachytherapy with transrectal ultrasound guidance-phantom experiments, J. Brachytherapy. 5 (March (1)) (2006) 14-26.

[5] B. Yusupov and S. Zlochiver, Biopsy Needle Localization Using Magnetic Induction Imaging Principles: A Feasibility Study, IEEE Trans. Biomed. Eng. 59(August (8)) (2012) 2330-2337.

[6] N. Hungr, M. Baumann, J Long, and J. Troccaz, A 3-D ultrasound robotic prostate brachytherapy system with prostate motion tracking, IEEE Trans. Robot.28(December (6)) (2012)1382-1397.

[7] C. Kim, D. Chang, D. Petrisor, G. Chirikjian, M. Han, and D. Stoianovici, Ultrasound probe and needle-guide calibration for robotic ultrasound scanning and needle targeting, IEEE Trans. Biomed. Eng. 60(February (6)) (2005)1728-1734.

[8] D. Stoianovici, C. Kim, G. Srimathveeravalli, P. Sebrecht, D. Petrisor, J. Coleman, S. B. Solomon, and H. Hricak, MRI-Safe robot for endorectal prostate biopsy, IEEE-ASME Trans Mechatronics. 19(August (4)) (2014)1289-1299.

[9] F. Rabbani, N. Stroumbakis, B. R. Kava, M. S. Cookson, and W. R. Fair, Incidence and clinical significance of false-negative sextant prostate biopsies, J. Urol. 159(April (4)) (1998)1247-1250.

[10] M. K. Terris, Strategies for repeat prostate biopsies, J. Curr. Urol. Rep. 10(May (3)) (2009)172-178.

[11] K. M. Pondman, J. J. Futterer, B. ten Haken, L. J. Schultze Kool, J.A.Witjes, T. Hambrock, K. J. Macura, and J. O. Barentsz, MR-guided biopsy of the prostate: An overview of techniques and a systematic review, J. Eur. Urol. 54(September (3)) (2008)517–527.

[12] G. L. McCreery, A. L. Trejos, M. D. Naish, R. V. Patel, and R. A. Malthaner, Feasibility of locating tumours in lung via kinaesthetic feedback, Int. J. Med. Robot. Comput. Assist. Surg. 4 (2008)58-68.

[13] A. L. Trejos, J. Jayander, M. T. Perri, M. D. Naish, R. V. Patel, and R. A. Malthaner, Robot-assisted tactile sensing for minimally invasive tumor localization, Int. J. Robot. Res. 28(May 9) (2009)1118-1133.

[14] H. Liu, D. P. Noonan, B. J. Challacombe, P. Dasgupta, L. D. Seneviratne, and K. Althoefer, Rolling Mechanical Imaging for Tissue Abnormality Localization during Minimally Invasive Surgery, IEEE Trans. Biomed. Eng. 57(February (2)) (2010) 404-414.

[15] M. T. Perri, A. L. Trejos, M. D. Naish, R. V. Patel, and R. A. Malthaner, Initial Evaluation of a Tactile/Kinesthetic Force Feedback System for Minimally Invasive Tumor Localization, IEEE/ASME Trans. Mechatronics, 15(December (6)) (2010) 925-931.

[16] Y. Kobayyashi, M. Suzuki, A. Kato, M. Hatano, K. Konishi, M. Hashizume, and M. G. Fujie, Enhanced targeting in breast tissue using a robotic tissue preloading-based needle insertion system, IEEE Trans. Robot. 28(December (6)) (2012) 1382-1397.

[17] S. Wellman, R. D. Howe, E. Dalton, and K. A. Kern, Breast tissue tiffness in compression is correlated to histological diagnosis, J. Tech. Rep, Harvard Biorobotics Laboratory, Cambridge, MA, (1999)1-15.

[18] Y. Kim, B. Ahn, J. W. Lee, K. H. Rha, and J Kim, Local property characterization of prostate glands using inhomogeneous modeling based on tumor volume and location analysis, J. Med. Biol. Eng. Comput. 51 (2013)197-205.

[19] V. Jalkanen, B. M. Andersson, A. Beigh, B. Ljungberg, and O. A. Lindahl, Indentation loading response of a resonance sensor-discriminating prostate cancer and normal tissue, J. Med. Eng. Technol. 37(August (7)) (2013)416-423.

[20] K. Hoyt, B. Castaneda, M. Zhang, P. Nigwekar, P.A. Santagnese, J.V. Joseph, J. Strang, D.J. Rubens, and K.J. Parker, Tissue elasticity properties as biomarker for prostate cancer, J. Cancer Biomark. 4(4-5) (2008) 213-225.

[21] P. N. Brett, T.J. Parker, A.J. Harrison, T.A. Thomas, and A. Carr, Simulation of resistance forces acting on surgical needles, in Proc. Inst. Mechanical Engineers, 211(4) (1997)335-347.

[22] P. N. Brett, A. J. Harrison, and T. A. Thomas, "Schemes for the identification of tissue types and boundaries at the tool point for surgical needles," IEEE Trans. Inform. Technol. Biomed. 4(March (1)) (2000)30-36.

[23] H. Kataoka, T. Washio, K. Chinzei, K. Mizuhara, C. Simone, and A. Okamura, Measurement of the tip and friction force acting on a needle during penetration, in Proc.Med. Image Comput. Comput. Assist. Interv. 2488 (2002)216-223.

[24] C. Simone and A. M. Okamura, Modeling of needle insertion forces for robot-assisted percutaneous therapy, in Proc. IEEE Int. Conf. Robot. Autom. 2 (2002)2085-2091.

[25] A. Okamura, C. Simone, and M. O'Leary, Force modeling for needle insertion into soft tissue," IEEE Trans. Biomed. Eng. 51(October (10)) (2004)1707-1716.

[26] A. Majewicz, S. P. Marra, M. G. Vledder, M. Lin, M. A. Choti, D. Y. Song, and A. M. Okamura, Behavior of tip-steerable needles in ex vivo and in vivo Tissue, IEEE Trans. Biomed. Eng. 59(February (10)) (2010)2705-2715.

[27] K. Yan, T. Podder, Y. Yu, T. Liu, C. W. Cheng, and W. S. Ng, Flexible Needle–Tissue Interaction Modeling With Depth-Varying Mean Parameter: Preliminary Study, IEEE Trans. Biomed. Eng. 56(February 2) (2009)255-262.

[28] K. Yan, L. Li, J. Joseph, D.R. Rubens, E.M. Messing, L. Liao, and Y. Yu, A real-time prostate cancer detection technique using needle insertion force and patient-specific criteria during percutaneous intervention, J. Med Phys. 36(July (7)) (2009) 3356-3362.